Heriot-Watt University
Research Gateway

Sparsity regularized optical interferometric imaging

Citation for published version:
Birdi, J, Repetti, A & Wiaux, Y 2017, Sparsity regularized optical interferometric imaging. in *Proceedings of SPARS 2017.* pp. 1-2.

Link:
Link to publication record in Heriot-Watt Research Portal

Document Version:
Peer reviewed version

Published In:
Proceedings of SPARS 2017

General rights
Copyright for the publications made accessible via Heriot-Watt Research Portal is retained by the author(s) and / or other copyright owners and it is a condition of accessing these publications that users recognise and abide by the legal requirements associated with these rights.

Take down policy
Heriot-Watt University has made every reasonable effort to ensure that the content in Heriot-Watt Research Portal complies with UK legislation. If you believe that the public display of this file breaches copyright please contact open.access@hw.ac.uk providing details, and we will remove access to the work immediately and investigate your claim.

Download date: 29. Nov. 2023

Sparsity regularized optical interferometric imaging

Jasleen Birdi, Audrey Repetti, and Yves Wiaux
Institute of Sensors, Signals and Systems, Heriot-Watt University, Edinburgh EH14 4AS, UK.

***Abstract*—Optical interferometry involves acquisition of under-sampled data related to the Fourier coefficients of the intensity image of interest, with missing phase information. It poses an ill-posed non-linear inverse problem for image recovery. In this context, for monochromatic imaging, a tri-linear data model was proposed in [1], leading to a non-negative non-linear least squares minimization problem, solved using a Gauss-Seidel method. In the recently submitted paper [2], we have developed a new robust method to improve upon the previous approach, by introducing a sparsity prior, imposed either by an ℓ_1 or a reweighted ℓ_1 regularization term. The resulting problem is solved using an alternating forward-backward algorithm, which is applicable to both smooth and non-smooth functions, and provides convergence guarantees in the non-convex context of interest. Moreover, our method presenting a general framework, we have extended it to hyperspectral imaging, where we have promoted a joint sparsity prior by an $\ell_{2,1}$ norm. Here we describe the proposed method and present simulation results to show its performance.**

I. Introduction

In the context of astronomical Optical Interferometry (OI), the measurements are performed by an array of antennas, such that each pair of antennas probes a spatial frequency in the Fourier domain (the u-v plane) of the image of interest, $\overline{\boldsymbol{x}} \in \mathbb{R}_+^N$. More precisely, for A antennas, an interferometer probes $A(A-1)/2$ spatial frequencies, leading to a sparse sampling of the u-v plane. For radio interferometry, these measurements correspond to complex visibilities. However, at optical wavelengths, the random phase fluctuations caused by the atmospheric turbulence leads to cancellation of the visibility values. Hence, the OI measurements consist of phase insensitive observables: power spectrum and bispectrum. On the one hand, $M_{\mathcal{P}}$ power spectrum measurements correspond to the squared moduli of these visibilities. On the other hand, $M_{\mathcal{B}}$ bispectrum measurements correspond to a triple product of three different complex visibilities, satisfying phase closure [3]. The loss of most of the phase information combined with the sparse sampling of the u-v plane poses a highly challenging task of image recovery in OI [3].

II. Proposed Approach

Each OI measurement can be represented by a triple product of the visibilities and the inverse problem can be written as:

$$\boldsymbol{y} = \left[(\mathsf{T}_1\overline{\boldsymbol{x}}) \cdot (\mathsf{T}_2\overline{\boldsymbol{x}}) \cdot (\mathsf{T}_3\overline{\boldsymbol{x}})\right] + \boldsymbol{\eta}, \tag{1}$$

where $\cdot$ denotes the Hadamard product, $\boldsymbol{y} \in \mathbb{C}^M$, with $M = M_{\mathcal{P}} + M_{\mathcal{B}}$, $\boldsymbol{\eta} \in \mathbb{C}^M$ is a realization of an additive i.i.d. Gaussian noise, and T_1, T_2, $\mathsf{T}_3 : \mathbb{R}^N \to \mathbb{C}^M$, are linear operators performing a discrete 2D Fourier transform, followed by selection of the Fourier coefficients to construct the measurements. To bring the linearity in the data model (1), as proposed in [1], we introduce $(\overline{\boldsymbol{u}}_1, \overline{\boldsymbol{u}}_2, \overline{\boldsymbol{u}}_3) \in (\mathbb{R}_+^N)^3$ such that $\overline{\boldsymbol{u}}_1 = \overline{\boldsymbol{u}}_2 = \overline{\boldsymbol{u}}_3 = \overline{\boldsymbol{x}}$ and reformulate the data model as:

$$\boldsymbol{y} = \left[(\mathsf{T}_1\overline{\boldsymbol{u}}_1) \cdot (\mathsf{T}_2\overline{\boldsymbol{u}}_2) \cdot (\mathsf{T}_3\overline{\boldsymbol{u}}_3)\right] + \boldsymbol{\eta}. \tag{2}$$

Using a Maximum a Posteriori approach, we estimate $(\overline{\boldsymbol{u}}_1, \overline{\boldsymbol{u}}_2, \overline{\boldsymbol{u}}_3)$ as a solution to

$$\underset{(\boldsymbol{u}_1,\boldsymbol{u}_2,\boldsymbol{u}_3)\in(\mathbb{R}^N)^3}{\text{minimize}} \frac{1}{2}\left\|\boldsymbol{y} - (\mathsf{T}_1\boldsymbol{u}_1) \cdot (\mathsf{T}_2\boldsymbol{u}_2) \cdot (\mathsf{T}_3\boldsymbol{u}_3)\right\|_2^2 + \sum_{p=1}^{3} r(\boldsymbol{u}_p)\,, \tag{3}$$

and define the final solution to be the mean over these estimations [2]. While the first term in (3) is the data fidelity term, $r\colon \mathbb{R}^N \to]-\infty, +\infty]$ is the regularization term incorporating *a priori* information on the target image $\overline{\boldsymbol{x}}$. In addition to the positivity constraint considered in [1], we propose to impose sparsity of the sought image in a dictionary $\Psi \in \mathbb{R}^{N\times J}$, with an ℓ_1 norm, or a reweighted ℓ_1 norm [4] such that the regularization term is given by:

$$(\forall \boldsymbol{x} \in \mathbb{R}^N) \quad r(\boldsymbol{x}) = \iota_{\mathbb{R}_+^N}(\boldsymbol{x}) + \mu\|\mathsf{W}\Psi^\dagger\boldsymbol{x}\|_1, \tag{4}$$

where $\iota_{\mathbb{R}_+^N}$ is the indicator function enforcing positivity of the sought image, $\mu \geq 0$ is the regularization parameter, and $\mathsf{W} \in \mathbb{R}^{J\times J}$ is a diagonal weighting matrix.

Exploiting the convexity of the sub-problems in (3) with respect to each of the variables $\boldsymbol{u}_1, \boldsymbol{u}_2, \boldsymbol{u}_3$, we propose to solve (3) using a block-coordinate forward-backward algorithm [5]. More precisely, this algorithm consists in solving sequentially for each of the variables $\boldsymbol{u}_1, \boldsymbol{u}_2, \boldsymbol{u}_3$, while keeping the other two fixed. The estimation of each variable $\left(\boldsymbol{u}_p\right)_{1\leq p\leq 3}$ is obtained by alternating between the gradient and proximity steps. The resulting algorithm is then guaranteed to converge to a critical point of the objective function in (3) [5].

III. Hyperspectral imaging

Keeping in mind the multi-wavelength imaging capabilities of modern optical interferometers, we extend our method for hyperspectral imaging. In order to reconstruct the image at L different wavelengths, we adopt the same methodolgy as developed for monochromatic case. To this purpose, we concatenate all the L spectral channels, and replace the variables and the operators in the monochromatic case with their hyperspectral counter-parts.

Here in addition to positivity, we exploit spatial sparsity of the sought image while favoring spectral continuity. Thus, we propose to regularize the problem with the joint sparsity prior using an $\ell_{2,1}$ norm [2], defined, for every $\boldsymbol{X} \in \mathbb{R}^{N\times L}$, by:

$$r(\boldsymbol{X}) = \iota_{\mathbb{R}_+^{N\times L}}(\boldsymbol{X}) + \mu \sum_{j=1}^{J} \left(\sum_{l=1}^{L} \left|[\Psi^\dagger \boldsymbol{x}_l]_j\right|^2 \right)^{1/2}, \tag{5}$$

where $\boldsymbol{X} = [\boldsymbol{x}_1, ..., \boldsymbol{x}_L]$ is a concatenation of the image vectors at each spectral channel, with $\boldsymbol{x}_l$ denoting the image vector at l-th spectral channel.

IV. Results and Conclusion

To assess the performance of the proposed method, we present simulation results considering the `LkH`α image [6], of size $N = 64^2$, with the realistic u-v coverage [2], where $M_{\mathcal{P}}$ = 72. It leads to only around 3.5 % sampling of the u-v plane. For each test, we vary $M_{\mathcal{B}}$, keeping $M_{\mathcal{P}}$ fixed, and perform simulations for 10 noise realizations. In terms of both SNR and visual quality, the results are shown in Fig. 1 and 2. For this highly undersampled u-v plane, the results indicate that for monochromatic imaging, promoting sparsity, especially by reweighted ℓ_1 regularization, gives promising results over positivity constrained case. Similarly, for the hyperspectral imaging, exploiting the joint sparsity significantly improves the reconstruction quality in comparison with single-channel reconstruction.

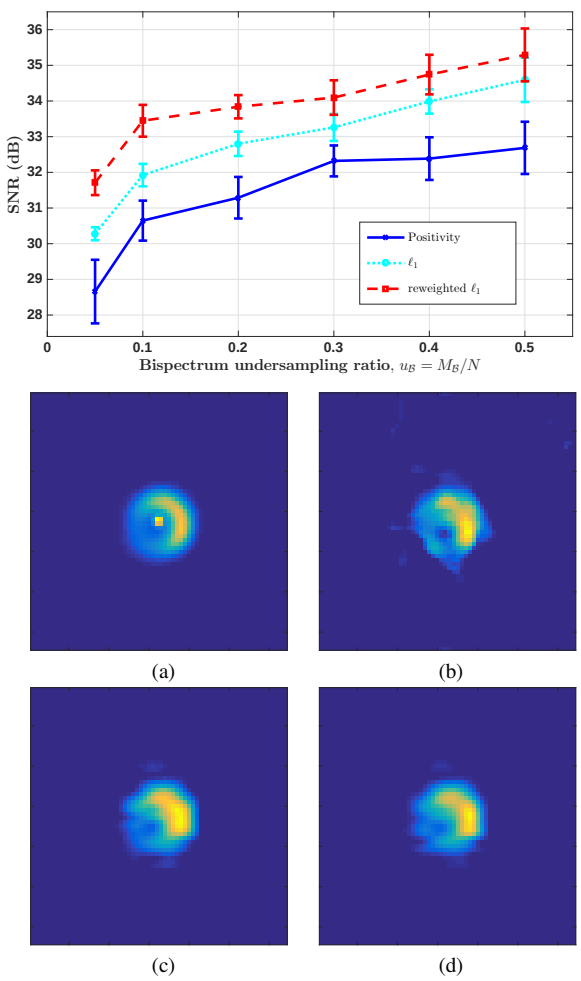

Fig. 1: Results for monochromatic imaging. First row: SNR graph depicting the comparison of average SNR values (over 10 simulations), and corresponding 1-standard-deviation error bars, for different regularization terms (input SNR = 30 dB). Second and third row: Reconstructed images obtained for $M_{\mathcal{B}}/N = 0.05$, corresponding to median SNR (over 10 simulations) are shown for different regularization terms - (a) True $\mathtt{LkH}\alpha$ image, (b) positivity constrained recovery, (c) recovery with ℓ_1 regularization, and (d) recovery with reweighted-ℓ_1 regularization. For these tests, Ψ is taken to be Daubechies 8 wavelet basis.

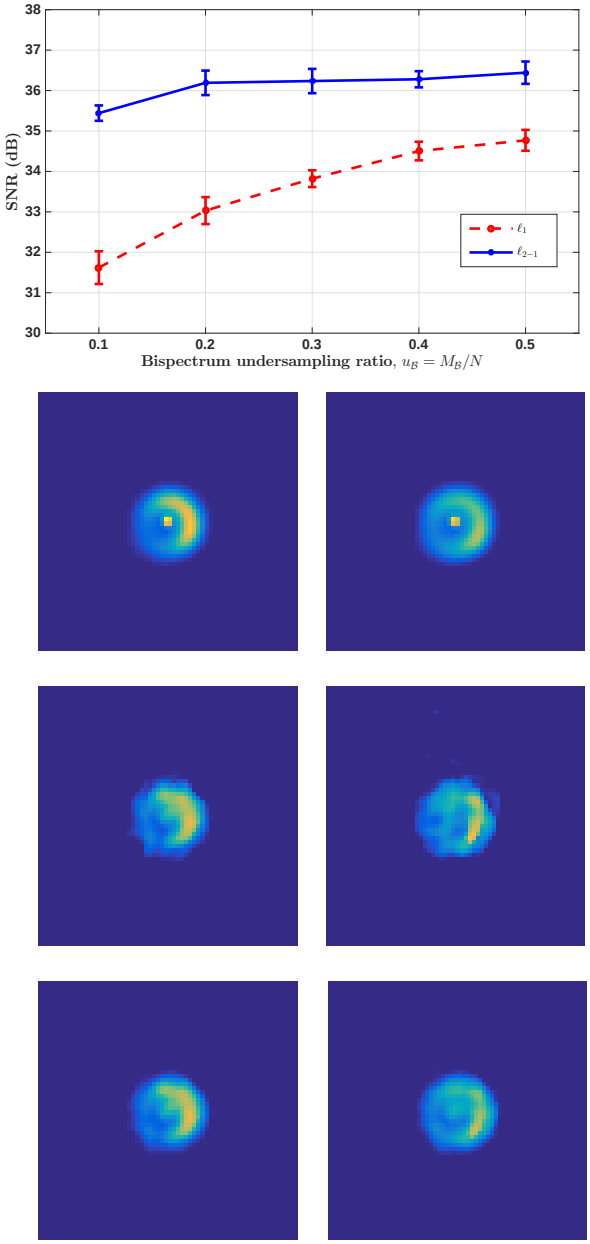

Fig. 2: Results for hyperspectral imaging for $L = 8$ spectral channels. First row: SNR graph depicting the comparison of the average SNR values (over 10 simulations) and corresponding 1-standard-deviation error bars, between single-channel reconstruction with ℓ_1 regularization and reconstruction by considering joint sparsity with $\ell_{2,1}$ regularization (input SNR = 30 dB). Second-fourth row: Left column shows the images corresponding to the first spectral channel, $l = 1$, right column shows the images corresponding to the last spectral channel, $l = 8$. In each column, original image (second row), reconstructed image with ℓ_1 regularization (third row) and reconstructed image with $\ell_{2,1}$ regularization (fourth row) are shown, respectively for $M_{\mathcal{B}}/N = 0.1$. For these tests, Ψ is taken to be the Identity matrix.

REFERENCES

[1] A. Auria, R. Carrillo, J. P. Thiran, and Y. Wiaux, "Tensor optimisation for optical-interferometric imaging," *Mon. Not. R. Astron. Soc.*, vol. 437, no. 4, pp. 2083–2091, 2014.

[2] J. Birdi, A. Repetti, and Y. Wiaux, "A regularized tri-linear approach for optical interferometric imaging," submitted to *Mon. Not. R. Astron. Soc.*, Sept. 2016, https://arxiv.org/abs/1609.00546.

[3] E. Thiébaut and J. F. Giovannelli, "Image reconstruction in optical interferometry," *IEEE Signal Process. Mag.*, vol. 27, pp. 97–109, 2010.

[4] E. J. Candès, M. B. Wakin, and S. P. Boyd, "Enhancing sparsity by reweighted ℓ_1 minimization," *J. Fourier Anal. Appl.*, vol. 14, no. 5, pp. 877–905, 2008.

[5] E. Chouzenoux, J.-C. Pesquet, and A. Repetti, "A block coordinate variable metric forward-backward algorithm," *J. Global Optim.*, vol. 66, no. 3, pp. 457–485, Nov. 2016.

[6] P. R. Lawson, W. D. Cotton, C. A. Hummel, J. D. Monnier, M. Y. Zhao, J. S., H. Thorsteinsson, S. C. Meimon, L. M. Mugnier, G. Le Besnerais, E. Thiébaut, and P. G. Tuthill, "An interferometry imaging beauty contest," vol. 5491, 2004, pp. 886–899.